PERGAMON

International Journal of Solids and Structures 37 (2000) 477–493

INTERNATIONAL JOURNAL OF SOLIDS and STRUCTURES

www.elsevier.com/locate/ijsolstr

Topology optimization of beam cross sections

Yoon Young Kim*, Tae Soo Kim

School of Mechanical and Aerospace Engineering, Seoul National University, San 56-1, Kwanak-Gu, Shinlim-Dong, Seoul 151-742, South Korea

Received 6 August 1998; in revised form 14 December 1998

Abstract

Perhaps, this paper reports the first successful applications of the topology optimization in the design of (thin-walled) beam sections. In particular, topologically different thin-walled beam cross sections can be obtained by the present approach, which is very useful in identifying the direction and location of stiffeners. In formulating the topology optimization problems, a simple power law is used for the relation between the density of an element with a hole and the mechanical properties of the element. The sensitivity of the torsional rigidity is obtained by developing a finite element model of a St. Venant torsion problem, and the Euler beam theory is used for the sensitivity analysis of the bending rigidities.

Keywords: Topology optimization; Cross-section; Torsion; Bending

1. Introduction

The beam cross section optimization problems have been very important as beams are widely used as efficient load-carrying structural members. Earlier investigations were based on analytic approaches (Banichuk, 1976; Banichuk and Karihaloo, 1976; Parbery and Karihaloo, 1977), but the optimization problems in more complicated geometries need to be solved numerically.

The section shape optimization based on the finite element formulation was carried out by Dems (1980) and Na et al. (1983). As a more efficient alternative method for section shape optimization, Mota Soares et al. (1984) and Gracia and Doblare (1988) used the boundary element method. Schramm and Pilkey (1993) developed a shape optimization technique using direct integration and B-splines. More literature on section optimization problems can be found in the references cited above. However, the aforementioned techniques are not applicable in obtaining (thin-walled) beam cross sections that are topologically different from original cross sections.

* Corresponding author. Fax: +82-2-883-1513.
E-mail address: yykim@plaza.snu.ac.kr (Y.Y. Kim)

0020-7683/00/$ - see front matter
PII: S0020-7683(99)00015-3

One important problem in beam section design is to find the location and direction of stiffeners, particularly in thin-walled beams. As the introduction of a stiffener in a closed beam may result in a topologically different cross section from the original cross section, the existing section shape optimization cannot be used. The purpose of this paper is to formulate a section topology optimization technique and apply it to various practical problems. In this work, the objective function is taken as a weighted sum of bending and torsional rigidities and a topology optimization technique is proposed to find the optimal cross section configuration.

The material homogenization concept (Bendsøe and Kikuchi (1988)) has been introduced to overcome the ill-posedness of optimal material layout problems. With this approach which converts the optimization problems into sizing optimization problems, the optimal material layout problems can be fairly relaxed. The present topology optimization technique is based on the technique and formulation developed for elastic bodies, not directly for beam structures (Bendsøe and Kikuchi, 1988; Guedes and Kikuchi, 1990; Suzuki and Kikuchi, 1991; Olhoff et al., 1991; Jog et al., 1994). A complete treatment of this subject and a number of related references can be found in Bendsøe (1995). In this optimization problem setting, the density of each element may be used as the design variable. A brief summary of the topology optimization that is necessary for the present analysis will be given in the next section.

The beam bending rigidity appearing in the objective function is based on the classical beam theory. The torsional rigidity is calculated by the finite element analysis of the St. Venant torsion problem for which the Prandtl stress function formulation is employed. To simplify the form of the objective function, an inequality relation stating that the torsional rigidity is always smaller than the mean bending rigidity is derived. The expression for the sensitivity of the torsional rigidity with respect to the design variable is explicitly obtained. Several cross sections including some practical ones are investigated as numerical examples. In particular, the direction and the location of a stiffener in a thin-walled closed beam section can be determined by applying the present topology optimization technique. The successful applications in this class of problems may be a major contribution of the present work.

2. Review of topology optimization using material density

In this section, a brief review of the topology optimization method using the material density as the design variable will be given. Fig. 1 illustrates an overview for a simple version of the topology optimization procedure. The design domain is uniformly discretized by finite elements having internal holes. The size of the hole governs the element or cell density and thus the homogenized mechanical

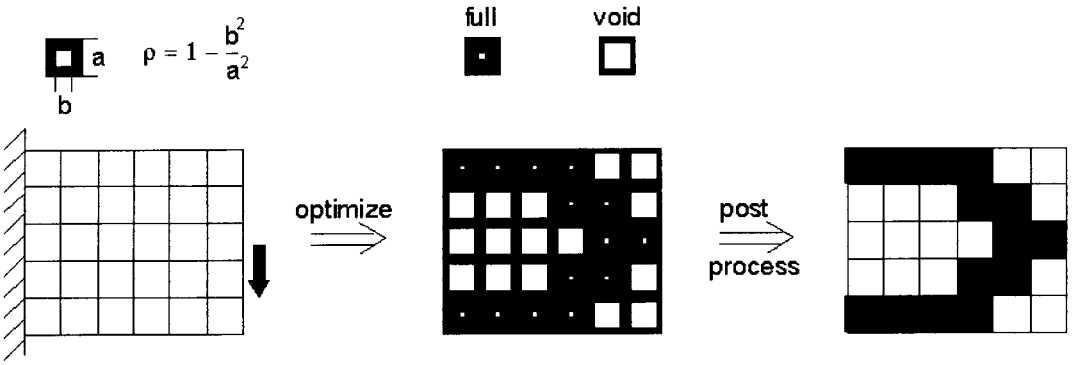

Fig. 1. Overview of the topology optimization procedure.

properties of the element. The density ρ appearing in Fig. 1 is defined as

$$\rho = 1 - \left(\frac{b}{a}\right)^2, \tag{1}$$

where a and b are the side lengths of the square element and hole, respectively.

In the homogenization-based topology optimization approach, the optimal element density distribution is obtained first. Then the obtained result is postprocessed to determine the optimal configuration for the given problem. Depending on the value of the element density, the element is regarded either full or void.

The rigorous homogenization technique (see e.g., Guedes and Kikuchi, 1990 and Bendsøe, 1995) can be used to find the relation between the density ρ and the material properties. However, a simple artificial relation between the density and the material properties can be also used in the topology optimization problems. Furthermore, it is assumed in this work that only Young's modulus E varies as the function of the density as

$$E = E(\rho) = E_0\rho^n \ (n = 2),\ 0<\rho\leq 1, \tag{2}$$

where E_0 is the Young's modulus of the material of the original element without any hole. Poisson's ratio ν and the area A are assumed to be independent of the density ρ. Therefore only the element stiffness changes as the hole size varies. For more rigorous treatments of this subject, see Bendsøe (1995). Fig. 2 illustrates graphically the present assumptions used in relating the density and the mechanical and geometrical properties.

The material and geometrical properties expressed as the functions of the element density will be used in determining the bending and torsional stiffness of a beam. The following sections derive the expressions for the bending and torsional rigidities that are needed for the topology optimization of beam cross sections.

3. Bending and torsional rigidities

Fig. 3 shows the general cross section of a beam along with a discretized model of it. The beam is subject to bending and twisting moments. The positive moment directions and the coordinate systems are also shown.

The bending rigidities, D_x, D_y and D_{xy}, may be found from the Euler–Bernouilli beam theory:

$$D_x = \int_A Ey^2\,\mathrm{d}A, \quad D_y = \int_A Ex^2\,\mathrm{d}A \quad \text{and} \quad D_{xy} = \int_A Exy\,\mathrm{d}A. \tag{3}$$

In Eq. (3), the Cartesian coordinate system (x, y) that has its origin at a centroid is defined as

$$x = X - X_\mathrm{c} \quad \text{and} \quad y = Y - Y_\mathrm{c}, \tag{4}$$

where (X, Y) is an arbitrarily located Cartesian coordinate system and X_c and Y_c are defined as

$$X_\mathrm{c} = \frac{\int_A EX\,\mathrm{d}A}{\int_A E\,\mathrm{d}A} \quad \text{and} \quad Y_\mathrm{c} = \frac{\int_A EY\,\mathrm{d}A}{\int_A E\,\mathrm{d}A}. \tag{5}$$

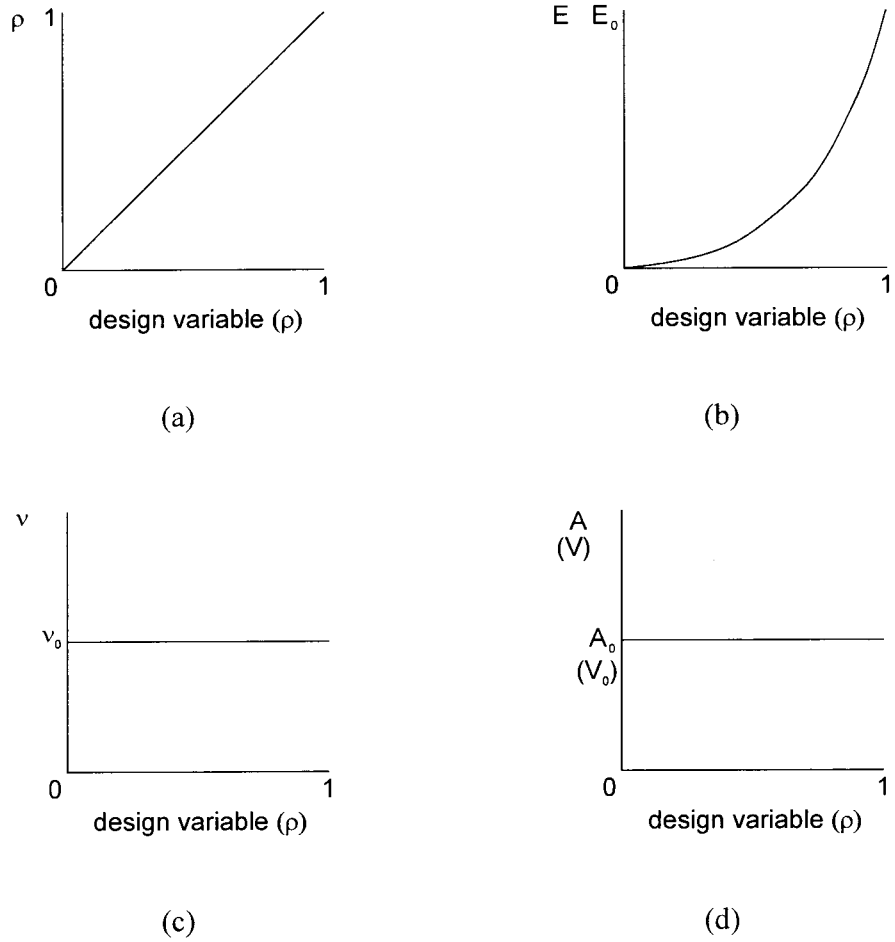

Fig. 2. The variation of the mechanical and geometrical properties as the function of the element density ρ: (a) ρ: Density of element; (b) E: Young's modulus; (c) ν: Poisson's ratio; (d) $A(V)$: Geometric area (volume).

The bending moments (M_X, M_Y) and the curvatures (κ_x, κ_y) are related as

$$\begin{Bmatrix} M_x \\ M_y \end{Bmatrix} = \begin{bmatrix} D_x & D_{xy} \\ D_{xy} & D_y \end{bmatrix} \begin{Bmatrix} \kappa_x \\ \kappa_y \end{Bmatrix}. \tag{6}$$

To carry out the topology optimization, we consider the beam cross section discretized with two-dimensional finite elements. Consequently, Eq. (3) must be rewritten as

$$D_x = \sum_{e=1}^{N_e} E \int_{A_e} y^2 \, dA, \quad D_y = \sum_{e=1}^{N_e} E \int_{A_e} x^2 \, dA \quad \text{and} \quad D_{xy} = \sum_{e=1}^{N_e} E \int_{A_e} xy \, dA, \tag{7}$$

where Young's modulus E is now regarded as the function of the element density ρ_e as in Eq. (2). The location of the centroid is rewritten as

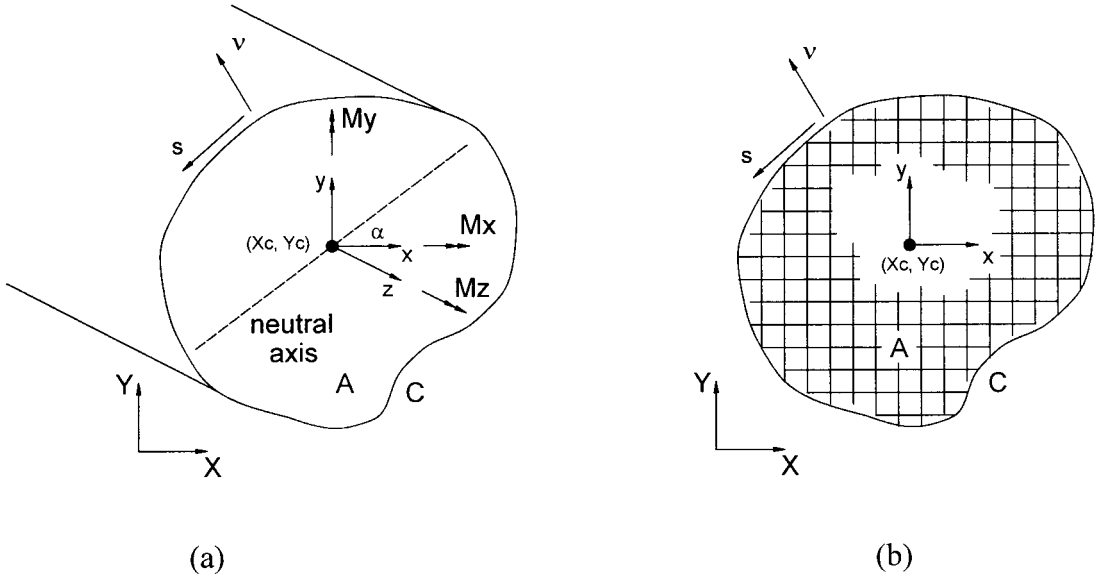

Fig. 3. (a) A beam under bending and torsional moment; (b) A discretized model of the cross section.

$$X_c = \frac{\sum_{e=1}^{N_e} E \int_{A_e} X \, dA}{\sum_{e=1}^{N_e} E \int_{A_e} dA} \quad \text{and} \quad Y_c = \frac{\sum_{e=1}^{N_e} E \int_{A_e} Y \, dA}{\sum_{e=1}^{N_e} E \int_{A_e} dA}, \tag{8}$$

where N_e is the total number of finite elements used to discretize the design domain.

Once the bending rigidities D_x, D_y and D_{xy} are determined, it is straightforward to find the maximum and minimum bending rigidities along the principal axes (Crandall et al., 1978):

$$D_{max} = D_{mean} + R_M \quad \text{and} \quad D_{min} = D_{mean} - R_M, \tag{9}$$

where D_{mean} is the mean bending rigidity defined as

$$D_{mean} = \frac{D_x + D_y}{2} \tag{10}$$

and R_M is given by

$$R_M = \sqrt{\frac{D_x + D_y}{2} + D_{xy}^2}. \tag{11}$$

Unlike the bending rigidity, the torsional rigidity for general cross sections must be obtained by solving a two-dimensional boundary value problem (see Timoshenko and Goodier, 1970; Sokolnikoff, 1955). The torsion problem may be formulated in terms of either the warping function or the Prandtl stress function, but the finite element analysis based on the Prandtl stress function formulation will be employed here as it gives a simpler expression for the torsional rigidity. Recent references on the solution of torsion problems may be found in Kim and Yoon (1997).

In the Prandtl stress formulation, the shear stress components are expressed as the derivatives of the stress function $\phi(x,y)$:

$$\sigma_{zx} = \frac{\partial \phi(x,y)}{\partial y} \quad \text{and} \quad \sigma_{zy} = \frac{\partial \phi(x,y)}{\partial x}, \tag{12}$$

where the stress function $\phi(x,y)$ must satisfy the following differential equation

$$\frac{\partial}{\partial x}\left(\frac{1}{G}\frac{\partial \phi}{\partial x}\right) + \frac{\partial}{\partial y}\left(\frac{1}{G}\frac{\partial \phi}{\partial y}\right) = -2\theta. \tag{13}$$

In Eq. (13), θ is the twist rate and $G(x, y)$ is the shear modulus. The traction-free beam wall condition along the boundary curve C may be given in terms of ϕ:

$$\frac{\mathrm{d}\phi}{\mathrm{d}s} = 0 \text{ or } \phi = \text{constant (0 for simply connected regions)}. \tag{14}$$

Once the solution to the stress function is found, the torsional rigidity is determined as (for simply connected regions)

$$D_z = M_z = 2\int_A \phi \, \mathrm{d}A \text{ with } \theta = 1. \tag{15}$$

The weak form of the Prandtl stress function formulation may be written as

$$\int_A \frac{1}{G}\nabla \upsilon \cdot \nabla \phi \, \mathrm{d}A = 2\theta \int_A \upsilon \, \mathrm{d}A, \tag{16}$$

where υ is an arbitrary function which lies in the admissible space ($\upsilon = 0$ on C). For the finite element analysis, the stress function ϕ is discretized, which may be written as

$$\phi = \mathbf{N}\Phi. \tag{17}$$

In Eq. (17), $\mathbf{N}$ is the displacement interpolation matrix and $\mathbf{\Phi}$ represents the column vector consisting of the nodal values of the stress function.

If a symbol $\mathbf{B}$ is introduced to designate the corresponding strain interpolation matrix, one can use Eq. (16) to obtain the following system of equations in the element level:

$$\mathbf{K}_\mathrm{e}\mathbf{\Phi}_\mathrm{e} = \mathbf{f}_\mathrm{e}, \tag{18}$$

where the element stiffness matrix $\mathbf{K}_\mathrm{e}$ and the load vector $\mathbf{f}_\mathrm{e}$ are

$$\mathbf{K}_\mathrm{e} = \int_{A_\mathrm{e}} \mathbf{B}_\mathrm{e}^T \mathbf{D}_\mathrm{e} \mathbf{B}_\mathrm{e} \, \mathrm{d}A \tag{19}$$

and

$$\mathbf{f}_\mathrm{e} = 2\theta \int_{A_\mathrm{e}} \mathbf{N}_\mathrm{e}^T \, \mathrm{d}A. \tag{20}$$

In Eq. (19), $\mathbf{D}_\mathrm{e}$ is the matrix defining the constitutive relation

$$\mathbf{D}_e = \begin{bmatrix} \frac{1}{G} & 0 \\ 0 & \frac{1}{G} \end{bmatrix}. \tag{21}$$

As for Young's modulus, the shear modulus is assumed to vary as

$$G = G(\rho_e) = G_0 \rho_e^n = \frac{E_0}{1(1+\nu)} \rho_e^n \ (n = 2). \tag{22}$$

Assembling Eq. (18) yields the final system equation:

$$\mathbf{K}\mathbf{\Phi} = \mathbf{f}, \tag{23}$$

where

$$\mathbf{K} = \sum_{e=1}^{N_e} \mathbf{K}_e, \tag{24a}$$

$$\mathbf{\Phi} = \sum_{e=1}^{N_e} \mathbf{\Phi}_e \tag{24b}$$

and

$$\mathbf{f} = \sum_{e=1}^{N_e} \mathbf{f}_e. \tag{24c}$$

The torsional rigidity D_z is now given by

$$D_z = 2 \sum_{e=1}^{N_e} \int_{A_e} \mathbf{N}_e \mathbf{\Phi}_e \, dA = 2 \sum_{e=1}^{N_e} \int_{A_e} \mathbf{N}_e \, dA \sum_{e=1}^{N_e} \mathbf{\Phi}_e. \tag{25}$$

Using Eqs. (24b) and (24c), the final expression for D_z is obtained as

$$D_z = \mathbf{f}^T \mathbf{\Phi} \text{ with } \theta = 1. \tag{26}$$

4. Optimization problem formulation

4.1. Objective function

In most beam section design problems, larger bending and torsional rigidities for a given mass constraint are desired. Unless specific values for the rigidities are specified, the minimization of R_M (half of the difference between the maximum and minimum principal values) and the maximization of D_{mean} (the mean value of the two principal values) may be sought for (see Eq. (9)). At the same time, the torsional rigidity D_z needs to be maximized.

Taking the element densities as the design variables, the objective function to minimize may be written as

$$f = -w_J D_z - w_M D_{\text{mean}} + w_I R_M + c_p \sum_{e=1}^{N_e} \rho_e(1-\rho_e) \tag{27}$$

and

$$0<\rho_e \le 1,\ e = 1,2\ldots,N_e, \tag{28}$$

where the w's represent weighting factors and the last term in Eq. (27) is a penalty function with a penalty constant c_p. Since the optimal shape of a cross section is extracted by the density distribution, it is always desirable to push the design variables towards the lower and upper limits 0 and 1 using the penalty function.

Instead of using Eq. (27) as the objective function, we propose to use a simpler function for the minimization problem:

$$f = -w_J D_z + w_I R_M + c_p \sum_{e=1}^{N_e} \rho_e(1-\rho_e). \tag{29}$$

The use of this function is justified because there exists an inequality relation between the mean bending rigidity D_{mean} and the torsional rigidity D_z such that

$$D_{\text{mean}} > D_z \text{ for } \nu > 0. \tag{30}$$

The proof of Eq. (30) is given in Appendix A.

4.2. Constraint

A typical constraint in structure optimization problems is a mass constraint. If the maximum allowable mass is denoted by M_0, the constraint equation is written simply as

$$\sum_{e=1}^{N_e} \int_{A_e} \rho_e \, dA - M_0 \le 0. \tag{31}$$

4.3. Sensitivity analysis

The sensitivities of the object function and the constraint equation need to be calculated during the optimization process. Therefore, the formula needed for the sensitivity calculations are derived explicitly below.

The sensitivity of the objective function in Eq. (29) with respect to the design variable ρ_e is simply

$$\frac{\partial f}{\partial \rho_e} = -w_J \frac{\partial D_z}{\partial \rho_e} + w_I \frac{\partial R_M}{\partial \rho_e} + c_p(1-2\rho_e). \tag{32}$$

The sensitivity of the quantity R_M in Eq. (32) is given by utilizing Eq. (11).

$$\frac{\partial R_M}{\partial \rho_e} = \frac{\left[(D_x - D_y)\left(\frac{\partial D_x}{\partial \rho_e} - \frac{\partial D_y}{\partial \rho_e}\right) + 4D_{xy}\frac{\partial D_{xy}}{\partial \rho_e}\right]}{2\sqrt{(D_x - D_y)^2 + 4D_{xy}^2}}, \tag{33}$$

where the sensitivity of the bending rigidities can be obtained by utilizing the definitions given in Eq. (7):

$$\frac{\partial D_x}{\partial \rho_e} = E' \int_{A_e} y^2 \, dA + \sum_{e=1}^{N_e} E \int_{A_e} 2y \frac{\partial y}{\partial \rho_e} \, dA,$$

$$\frac{\partial D_y}{\partial \rho_e} = E' \int_{A_e} x^2 \, dA + \sum_{e=1}^{N_e} E \int_{A_e} 2x \frac{\partial x}{\partial \rho_e} \, dA$$

and

$$\frac{\partial D_{xy}}{\partial \rho_e} = E' \int_{A_e} xy \, dA + \sum_{e=1}^{N_e} E \int_{A_e} \left(x \frac{\partial y}{\partial \rho_e} + y \frac{\partial x}{\partial \rho_e} \right) dA. \tag{34}$$

In Eq. (34), $(\,)'$ denotes differentiation with respect to ρ_e. The sensitivities of x and y should not be neglected in Eq. (34). Using Eqs. (4) and (8),

$$\frac{\partial x}{\partial \rho_e} = -\frac{\partial X_c}{\partial \rho_e} = \frac{E' \int_{A_e} dA \sum_{e=1}^{N_e} E \int_{A_e} X \, dA - E' \int_{A_e} X \, dA \sum_{e=1}^{N_e} E \int_{A_e} dA}{\left(\sum_{e=1}^{N_e} E \int_{A_e} dA \right)^2}$$

and

$$\frac{\partial y}{\partial \rho_e} = -\frac{\partial Y_c}{\partial \rho_e} = \frac{E' \int_{A_e} dA \sum_{e=1}^{N_e} E \int_{A_e} Y \, dA - E' \int_{A_e} Y \, dA \sum_{e=1}^{N_e} E \int_{A_e} dA}{\left(\sum_{e=1}^{N_e} E \int_{A_e} dA \right)^2}. \tag{35}$$

The sensitivity of the torsional rigidity in Eq. (32) can be found by utilizing Eq. (26).

$$\frac{\partial D_z}{\partial \rho_e} = \frac{\partial (\mathbf{f}^T \mathbf{\Phi})}{\partial \rho_e} = \mathbf{f}^T \frac{\partial \mathbf{\Phi}}{\partial \rho_e} = \mathbf{\Phi}^T \mathbf{K} \frac{\partial \mathbf{\Phi}}{\partial \rho_e}. \tag{36}$$

To simplify Eq. (36), Eq. (23) is differentiated with respect to the design variable and premultiplied by $\mathbf{\Phi}^T$:

$$\mathbf{\Phi}^T \mathbf{K} \frac{\partial \mathbf{\Phi}}{\partial \rho_e} = -\mathbf{\Phi}^T \frac{\partial \mathbf{K}}{\partial \rho_e} \mathbf{\Phi}. \tag{37}$$

Substituting Eq. (37) into Eq. (36) yields

$$\frac{\partial D_z}{\partial \rho_e} = -\mathbf{\Phi}^T \frac{\partial \mathbf{K}}{\partial \rho_e} \mathbf{\Phi} = -\mathbf{\Phi}_e^T \frac{\partial \mathbf{K}_e}{\partial \rho_e} \mathbf{\Phi}_e = \frac{G'}{G} \mathbf{\Phi}_e^T \mathbf{K}_e \mathbf{\Phi}_e. \tag{38}$$

Note that the sensitivity of the torsional rigidity with respect to the density of the e-th finite element can be computed within the element level.

The sensitivity of the constraint in Eq. (31) is straightforward to obtain:

$$\frac{\partial}{\partial \rho_e}\left(\sum_{e=1}^{N_e}\int_{A_e}\rho_e\,dA - M_0\right) = \frac{\partial}{\partial \rho_e}\int_{A_e}\rho_e\,dA = \int_{A_e} dA. \tag{39}$$

From the result given by Eq. (39), the sensitivity of the constraint equation with respect to the density of the e-th element is nothing but the element area.

For the numerical analysis of the present optimization problem, the method of feasible direction (see Haftka and Gürdal, 1992 and Vanderplaats, 1984a) is used. (*ADS* (Vanderplaats, 1984b) is used for the actual numerical work). The values of the design variables are updated utilizing the sensitivity results given above. When converging results are obtained, the design variables take on the values close to the limit values. This is due to the penalty term added in the definition of the objective function. Subsequently, clearly identifiable section shapes may be obtained.

5. Numerical examples

As the application examples of the present topology optimization in the beam section design, we consider three cases. The first one is a simple case in which a section bounded by a square profile is to be optimized. (For all the optimization problems discussed in this section, the objective function f in Eq. (29) will be minimized). This case serves to check the validity of the present analysis. The second case deals with the reinforcement of a thin-walled cross section, and the resulting reinforced cross section has the same topology as the original one. The third case also deals with thin-walled beam section reinforcement, but the resulting cross sections can be topologically different from the original one. This is the case that most other optimization techniques including the shape optimization technique cannot handle. Perhaps, this is the example for which the present topology optimization contributes in a unique way to the thin-walled beam section design in comparison with existing approaches.

5.1. Verification problem

To verify the validity of the present method, a simple design optimization problem is considered. Fig. 4 shows the domain for the section design. The problem is to find the section shape to minimize the function f in Eq. (29) subject to different mass constraints. In this case, we take $w_J = 1$ and $w_I = 0$ as symmetric cross sections will be sought for. The optimal section configurations obtained from the present analysis are shown in Fig. 5.

As expected, the strict limitation on the total mass yields a thin-walled section close to a hollow circular cross section. To obtain the configuration shown in Fig. 5, the initial design variables are taken to be constant with $\rho_e = 0.1$. During the iterations of the design optimization, the design variables are pushed towards to the values close to either 0 or 1.

5.2. Thin-walled section reinforcement: resulting in variable beam thickness

As the second case, the problem of the reinforcement of a thin-walled beam section is considered. The thin-walled beam section is shown in Fig. 6. The goal is to find a cross section with the maximum rigidity subject to a mass constraint. Two results obtained from the present topology optimization technique are shown in Fig. 7. The mass constraint ratio is set equal to 20% of the design domain. Depending on the values of the weighting factors, somewhat differently reinforced beam sections are

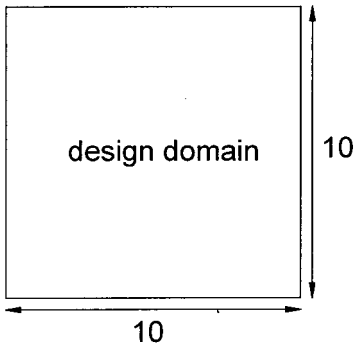

Fig. 4. Section design domain (dimensionless units are used for convenience).

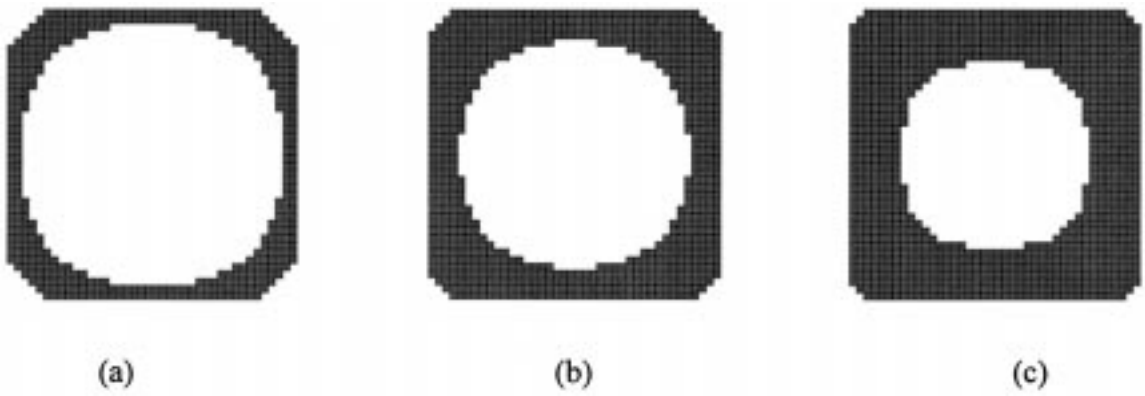

Fig. 5. Optimized cross sections: (a) 30% mass constraint; (b) 50% mass constraint; (c) 60% mass constraint.

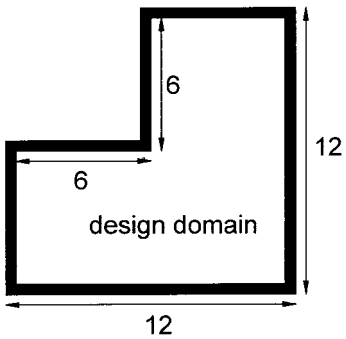

Fig. 6. The design domain for a thin-walled cross section.

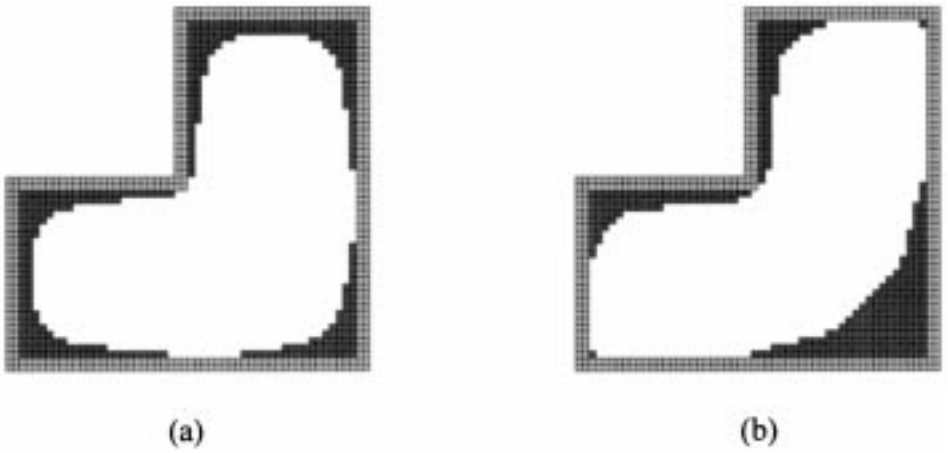

Fig. 7. Optimized cross sections (20% mass constraint): (a) $w_J = 1.0$ and $w_I = 0.0$; (b) $w_J = 1.0$ and $w_I = 0.02$.

obtained. The convergence history is shown in Fig. 8, and the final values of the bending and torsional rigidities listed in Table 1 show the sectional characteristics of the optimized sections.

From the optimized section shapes shown in Fig. 7, one may estimate the optimal distribution of the cross section wall thickness. The present observation is not only interesting but also very useful in a wide class of thin-walled beam section design problems. As shall be seen in the next example, the topology optimization technique also gives a reinforced beam section that is topologically different from the original section. Therefore, a unified treatment of (thin-walled) section design may be carried out within the same frame of the section topology optimization.

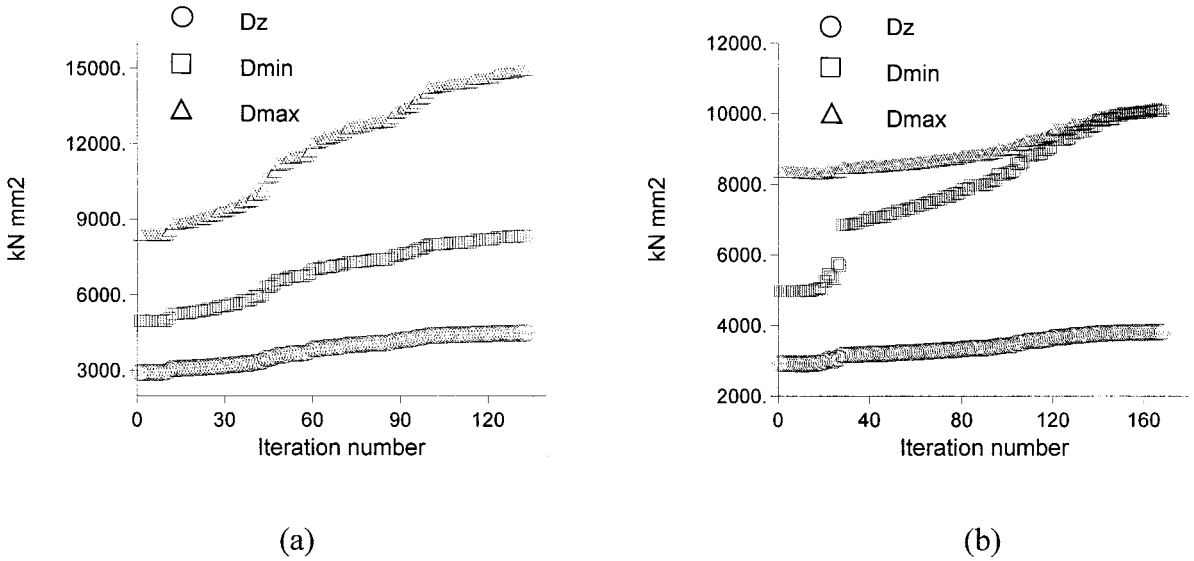

Fig. 8. Convergence history for the results shown in Fig. 7: (a) $w_J = 1.0$ and $w_I = 0.0$; (b) $w_J = 1.0$ and $w_I = 0.02$.

Table 1
Change of the cross section rigidities ($E = 13\ \mathrm{kN\ mm^{-2}}$, $\nu = 0.3$)

20% constraint	$w_J = 1.0$ and $w_I = 0.0$		$w_J = 1.0$ and $w_I = 0.02$	
	Initial	Final	Initial	Final
D_z (kN mm^{-2})	2910.4	4488.4	2910.4	3805.2
$D_{\min}$ (kN mm^{-2})	4963.1	8327.7	4963.1	10074
$D_{\max}$ (kN mm^{-2})	8308.6	14870	8308.6	10095

5.3. Thin-walled section reinforcement: resulting in different topology

There are some instances in which the external profile of a thin-walled beam cross section cannot be changed although the section rigidity needs to be increased. For instance, when a beam needs to be assembled to other structural elements which are already manufactured or whose profiles are difficult to change, the beam section profile may not be changed, either. In this case, only stiffening inside the beam cross section may be allowed.

As a specific example, we consider a section shown in Fig. 9 where the beam profile marked by thick solid lines is assumed not be altered because of its assembly requirement with adjacent structural components. The goal of this problem is to find the optimal location and direction of a stiffener in the design domain that lies inside the cross section profile.

To find the optimal location and direction of a stiffener, we apply the topology optimization technique formulated in the previous section. Two sets of weighting factors are considered with the 40% mass constraint. The section shapes obtained from the present analysis are shown in Fig. 10. The convergence history is also shown in Fig. 11. Table 2 compares the sectional rigidities of the initial section having a uniform density distribution with those of the final optimal cross section. The optimal location and the direction of a stiffener can be identified from the optimal shape shown in Fig. 10. This indeed demonstrates the usefulness of the present topology optimization technique in the thin-walled beam section stiffener design. Without this approach, optimal stiffening configurations would be difficult to find.

In topology optimization, utilizing the artificial material density model as used in this work, the solution usually depends on the mesh-size. However, the present problems are insensitive to meshing size: compare Fig. 10(a) and Fig. 12. The result shown in Fig. 12 is obtained with the half size of the original mesh shown in Fig. 10(a). The solution insensitiveness to mesh-size in this problem is partly because of the use of the penalty function introduced in the objective function.

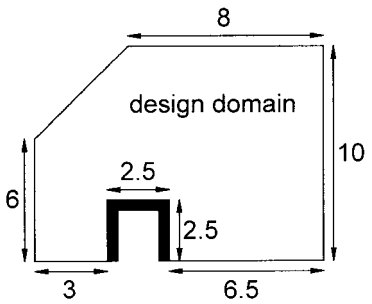

Fig. 9. Initial design domain with a geometric constraint.

Fig. 10. Optimized cross sections (40% mass constraint): (a) $w_J = 1.0$ and $w_I = 0.0$; (b) $w_J = 1.0$ and $w_I = 0.4$.

We have also considered the case with a tighter mass constraint, namely a 25% mass constraint. The results are depicted in Fig. 13, but they appear somewhat impractical. However, it is worth noting that the candidate location and direction of an optimal stiffener may be predicted quite well even with these results.

6. Conclusions

A new topology optimization technique of beam cross sections is proposed in this paper. It is demonstrated that a unified treatment of optimal section profile design, wall-thickness distribution and section topology configuration can be achieved using the present technique. Among others, optimal

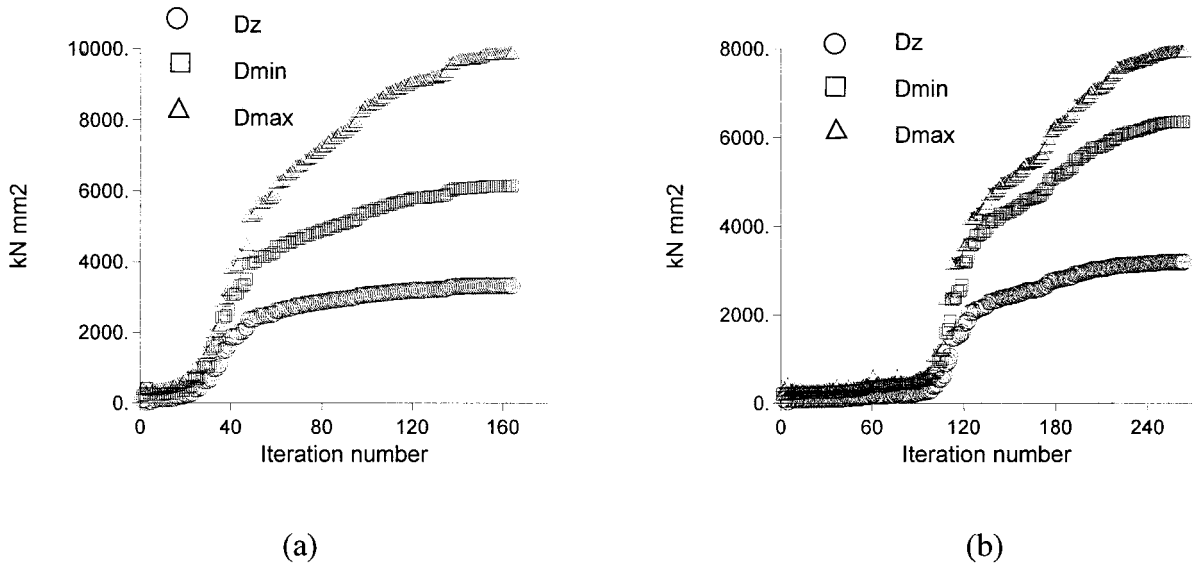

Fig. 11. Convergence history for the results shown in Fig. 10: (a) $w_J = 1.0$ and $w_I = 0.0$; (b) $w_J = 1.0$ and $w_I = 0.4$.

Table 2
Cross sectional rigidities before and after optimization; The results before optimization are those obtained from the sections with uniform density distribution ($E = 13\ \text{kN mm}^{-2}$, $\nu = 0.3$)

40% constraint	$w_J = 1.0$ and $w_I = 0.0$		$w_J = 1.0$ and $w_I = 0.4$	
	Initial	Final	Initial	Final
D_z (kN mm^{-2})	86.385	3318.8	86.385	3189.5
$D_{\min}$ (kN mm^{-2})	198.87	6139.8	198.87	6357.6
$D_{\max}$ (kN mm^{-2})	360.62	9831.7	360.62	7900.6

Fig. 12. Optimized cross section with the half size of the original mesh used for Fig. 10(a).

Fig. 13. Optimized cross sections (25% mass constraint): (a) $w_J = 1.0$ and $w_I = 0.0$; (b) $w_J = 1.0$ and $w_I = 0.4$.

stiffening direction and location in thin-walled section can be found with the present approach; this would be difficult to achieve with any other existing approaches.

Acknowledgements

Acknowldegements: The first author wishes to acknowledge the financial support of Korea Research Foundation made in the program of 1997. This work was completed during his stay at Stanford University and he thanks the Division of Mechanics and Computation, Stanford University.

Appendix A

In order to prove Eq. (30), it is convenient to formulate the torsion problem in terms of the warping function ψ that satisfies the following equation and boundary condition:

$$\frac{\partial}{\partial x}\left[G\left(\frac{\partial \psi}{\partial x}-y\right)\right]+\frac{\partial}{\partial y}\left[G\left(\frac{\partial \psi}{\partial y}+x\right)\right]=0, \tag{A1}$$

$$\left(\frac{\partial \psi}{\partial x}y\right)\frac{\mathrm{d}y}{\mathrm{d}s}-\left(\frac{\partial \psi}{\partial y}+x\right)\frac{\mathrm{d}x}{\mathrm{d}s}=0 \quad \text{or} \quad \frac{\mathrm{d}\psi}{\mathrm{d}\nu}=y\nu_x-x\nu_y \text{ on } C. \tag{A2}$$

In terms of the warping function ψ, the torsional rigidity can be written as (see Timoshenko and Goodier, 1970 or Sokolnikoff, 1955)

$$D_z=\int_A G\left(x^2+y^2+x\frac{\partial \psi}{\partial y}-y\frac{\partial \psi}{\partial x}\right)\mathrm{d}A. \tag{A3}$$

Now applying the divergence theorem to the integral involving ψ in Eq. (A3) and using Eq. (A2) gives

$$\begin{aligned} D_z &= \int_A G(x^2+y^2)\mathrm{d}A+\int_A \psi\left(y\frac{\partial G}{\partial x}-x\frac{\partial G}{\partial y}\right)\mathrm{d}A-\int_C G\psi\left(y\frac{\partial y}{\partial s}+x\frac{\partial x}{\partial s}\right)\mathrm{d}s \\ &= \int_A G(x^2+y^2)\mathrm{d}A+\int_A \psi\left(y\frac{\partial G}{\partial x}-x\frac{\partial G}{\partial y}\right)\mathrm{d}A-\int_C G\psi\left(y\frac{\partial \psi}{\partial x}\frac{\mathrm{d}y}{\mathrm{d}s}-\frac{\partial \psi}{\partial y}\frac{\mathrm{d}x}{\mathrm{d}s}\right)\mathrm{d}s. \end{aligned} \tag{A4}$$

Reapplying the divergence theorem to the last integral in Eq. (A4) and then substituting Eq. (A1) yields the following result:

$$\begin{aligned} D_z &= \int_A G(x^2+y^2)\mathrm{d}A+\int_A \psi\left(y\frac{\partial G}{\partial x}-x\frac{\partial G}{\partial y}\right)\mathrm{d}A-\int_A \frac{\partial}{\partial x}\left(G\psi\frac{\partial \psi}{\partial x}\right)+\frac{\partial}{\partial y}\left(G\psi\frac{\partial \psi}{\partial y}\right)\mathrm{d}A \\ &= \int_A G(x^2+y^2)\mathrm{d}A-\int_A G\left[\left(\frac{\partial \psi}{\partial x}\right)^2+\left(\frac{\partial \psi}{\partial y}\right)^2\right]\mathrm{d}A. \end{aligned} \tag{A5}$$

The mean bending rigidity D_{mean} can be explicitly written when Eqs. (7) and (10) and the relation $E=2E/(1+\nu)$ are utilized:

$$D_{\text{mean}} = \frac{1}{2}\int_A E(x^2+y^2)\mathrm{d}A = (1+\nu)\int_A G(x^2+y^2)\mathrm{d}A. \tag{A6}$$

It is then straightforward to show Eq. (30) from the following result:

$$D_{\text{mean}} = -D_z = \nu\int_A G(x^2+y^2)\mathrm{d}A + \int_A G\left[\left(\frac{\partial\psi}{\partial x}\right)^2+\left(\frac{\partial\psi}{\partial y}\right)^2\right]\mathrm{d}A. \tag{A7}$$

References

Banichuk, N.V., 1976. Optimization of elastic bars in torsion. Int. J. Solids and Struct. 12, 275–286.

Banichuk, N.V., Karihaloo, B.L., 1976. Minimum-weight design of multipurpose cylindrical bars. Int. J. Solids and Struct. 12, 267–273.

Bendsøe, M.P., 1995. Optimization of Structural Topology, Shape and Material. Springer, Berlin.

Bendsøe, M.P., Kikuchi, N., 1988. Generating optimal topologies in structural design using a homogenization method. Comp. Meth. Appl. Mech. Engrg. 71, 197–224.

Crandall, S.H., Dahl, N.C., Lardner, T.J., 1978. An Introduction to the Mechanics of Solids, 2nd ed. McGraw–Hill, New York.

Dems, K., 1980. Multiparameter shape optimization of elastic bars in torsion. Int. J. Numer. Meth. Engrg. 15, 1517–1539.

Gracia, L., Doblare, M., 1988. Shape optimization of elastic orthotropic shafts under torsion by using boundary elements. Comput. Struct. 30, 1281–1291.

Guedes, J.M., Kikuchi, N., 1990. Preprocessing and postprocessing for materials based on the homogenization method with adaptive finite element methods. Comp. Meth. Appl. Mech. Engrg. 83, 143–198.

Haftka, R.T., Gürdal, Z., 1992. Elements of Structural Optimization, 3rd ed. Kluwer Academic Publishers, London.

Jog, C.S., Haber, R.B., Bendsøe, M.P., 1994. Topology design with optimized, self-adaptive materials. Int. J. Numer. Meth. Engrg. 37, 1323–1350.

Kim, Y.Y., Yoon, M.S., 1997. A modified Fourier series method for the torsion analysis of bars with multiply-connected cross sections. Int. J. Solids and Struct. 34, 4327–4337.

Mota Soares, C., Rodrigues, H.C., Oliveira Faria, L.M., Haug, E.J., 1984. Optimization of the geometry of shafts using boundary elements. J. of Mech. Transms. Automa. Des. 106, 199–202.

Na, M.S., Kikuchi, N., Taylor, J.E., 1983. Shape optimization for elastic torsion bars. In: Optimization Methods in Structural Design. Bibliographisches Institut AG, Zürich, pp. 216–233.

Olhoff, N., Bendsøe, M.P., Rasmussen, J., 1991. On CAD-integrated structural topology and design optimization. Comp. Meth. Appl. Mech. Engrg. 89, 259–279.

Parbery, R.D., Karihaloo, B.L., 1977. Minimum-weight design of hollow cylinders for given lower bounds on torsional and flexural rigidities. Int. J. Solids and Struct. 13, 1271–1280.

Schramm, U., Pilkey, W.D., 1993. Structural shape optimization for the torsional problem using direct integration and B-splines. Comp. Meth. Appl. Mech. Engrg. 107, 251–268.

Sokolnikoff, I.S., 1956. Mathematical Theory of Elasticity, 2nd ed. McGraw–Hill, New York.

Suzuki, K., Kikuchi, N., 1991. A homogenization method for shape and topology optimization. Comp. Meth. Appl. Mech. Engrg. 93, 291–318.

Timoshenko, S.P., Goodier, J.N., 1970. Theory of Elasticity, 3rd ed. McGraw–Hill, New York.

Vanderplaats, G.N., 1984a. Numerical Optimization Techniques for Engineering Design. McGraw–Hill, New York.

Vanderplaats, G.N., 1984b. ADS — A Fortran Program for Automated Design Synthesis NASA CR 172460.